Internal Rotation of the Methyl Groups in the *t*-Butyl Radical as Studied by ESR

Souichi Kubota, Michio Matsushita,# Tadamasa Shida,* Atieh Abu-Raqabah,† Martyn C. R. Symons,*,†† and Jane L. Wyatt†

Department of Chemistry, Faculty of Science, Kyoto University, Kyoto 606-01

†Department of Chemistry, The University of Leicester, Leicester LE1 7RH, U.K.

††Department of Chemistry and Biological Chemistry, University of Essex, Colchester CO4 3SQ, U.K.

(Received June 24, 1994)

The ESR spectrum of the *t*-butyl radical in a rigid matrix is observed at temperatures between 6.6 and 70 K. At temperatures below about 50 K equally spaced nineteen lines are observed which is associated with the tunneling rotation of the three methyl groups. By the analysis of the spectral pattern at a low temperature of 6.6 K the pairwise interaction potential of the internal rotation, if any, is deduced to be proportional to $\cos\theta_i \cos\theta_j$ where θ_i and θ_j are the internal rotation angles of two methyl groups. By the simulation of the spectral change with temperature the thermal activation energy for the internal rotation is estimated to be 6±2 kJ mol^{-1}.

ESR spectra of some radicals having a single methyl group adjacent to the odd electron center show seven lines with an intensity ratio of 1 : 1 : 1 : 2 : 1 : 1 : 1 at low temperatures which is well understood in terms of the coupling of the internal rotation of the methyl group and the hyperfine interaction.[1—3] As for the radicals having multiple methyl groups, however, there are no ESR studies focusing on this coupling except for the study of the radical cation of dimethyl ether.[4] In this work we have studied a three-methyl group system, that is, the *t*-butyl radical.[5,6] The study is a straightforward extension of the previous study on the two-methyl group system.[4] A difference between the two systems is that in the *t*-butyl radical the umbrella motion of the three methyl groups is conceivable. However, the present work will not deal with the effect of the umbrella motion because the observed hyperfine structure is explicable in terms of the methyl protons and because the possible additional structure due to the umbrella motion is not resolved. A piece of evidence in favor of planarity has been given.[6] Also, as in the case of the dimethyl ether[4] the overall rotation of the *t*-butyl radical is ignored because of the rigidity of the low temperature matrix employed. The thermally-induced rotation of the methyl groups is also analyzed.

Experimental

t-Butyl chloride was dissolved in CD_3OD to a concentration of 1 M (1 M=1 mol dm^{-3}) and sealed off in a Suprasil cell after degassing. The solution was γ-irradiated at 77 K to a dose of 1.47×10^3 Gy (1 Gy=1 J kg^{-1}). The ESR measurement was carried out with JEOL RE-2X spectrometers at Kyoto and at Leicester. An Air Products LTR-3 liquid helium transfer Heli-Tran refrigerator was used for the measurement at various temperatures. A calibrated Au–Fe/chromel thermocouple was used for the temperature determination.

Experimental Results

The ESR spectra of γ-irradiated solutions were measured at 6.6—70 K. Typical spectra are shown in Figs. 1 and 2 along with the simulated spectra. The general spectral change with temperature can be summarized as follows. The spectrum at 6.6 K in Fig. 1 is regarded as consisting of nineteen lines in reference to the simulated spectrum. The scaled-off signal at 3250—3280 G (1 G=10^{-4} T) is due to the byproduced CD_2OD radical which masks approximately three out of the nineteen lines. As the temperature was raised to ca.30 K, every other line became weaker. At temperatures of ca.30—ca.45 K the spectral pattern appeared to be intermediate between the patterns below ca.30 K and above ca.45 K. At above ca.50 K the ten-line feature became dominant and at the final temperature of 70 K a ten-line spectrum with the binomial intensity ratio appeared.

Spectral Analysis

The Symmetry of the System. For the analysis of the dynamical feature of the methyl groups the Permutation-Inversion (PI) group theoretic analysis is

#Present address: The Institute for Molecular Science, Okazaki 444, Japan.

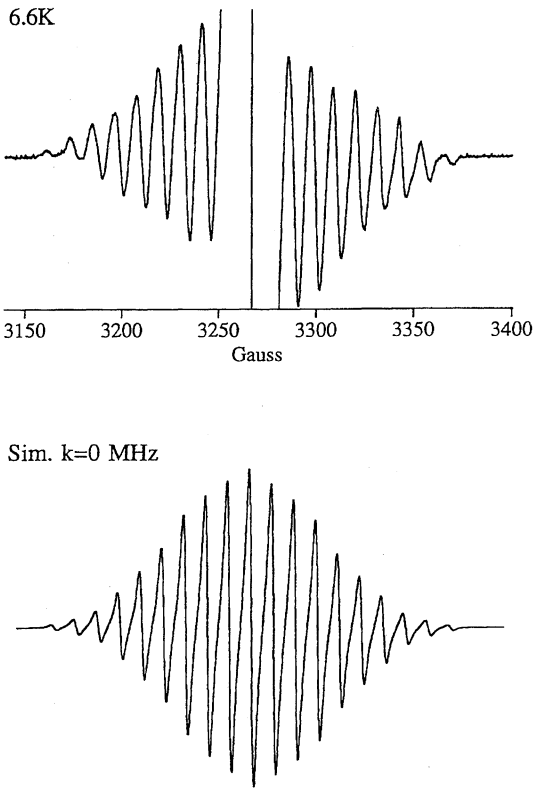

Fig. 1. ESR spectra of the *t*-butyl radical observed at 6.6 K for γ-irradiated deuterated methanol containing *t*-butyl chloride as the solute (upper) and simulated by assigning the jumping rate k (see text) as zero (lower).

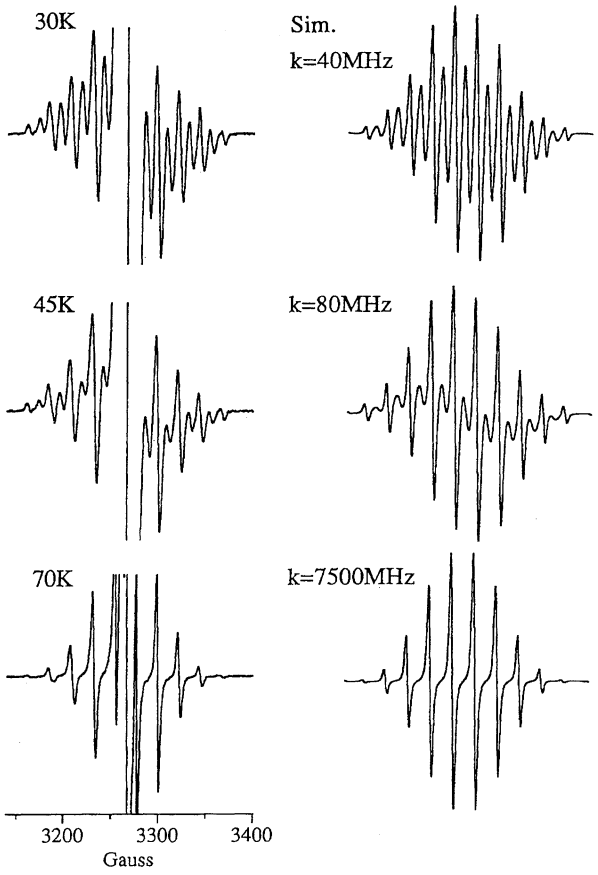

Fig. 2. ESR spectra of the *t*-butyl radical observed at several temperatures (left) and simulated with the jumping parameters indicated (right).

appropriate.[1,7,8] The "feasible" PI operations of a rotating methyl group are the cyclic permutation of the three protons.[1] The symmetry group of such a system, denoted by G_3, consists of the three "feasible" operations, $G_3=\{E,(123),(132)\}$, where the three protons are numbered 1,2, and 3. Since there are three methyl groups in the *t*-butyl radical, the symmetry group of the radical is the direct product group of the three G_3 groups. The direct product group will be called G_{27} because it has 27 elements. Since G_3 is isomorphic to the point group C_3, we will make use of the notations of the irreducible representations A, Ea, and Eb of C_3. Accordingly, the symmetry species of the G_{27} group will be denoted by AAA, AAEa, AEaEb, and so on.

The Hamiltonian and the Basis Functions. The relevant Hamiltonian consists of the internal rotation of the methyl groups and the spin part as in Eq. 1.

$$\mathscr{H}=\mathscr{H}_R+\mathscr{H}_S. \quad (1)$$

The rotational part is approximated by Eq. 2 as in the previous work,[4]

$$\mathscr{H}_R=-\frac{\hbar^2}{2I_{CH_3}}\left(\frac{\partial^2}{\partial\theta_1^2}+\frac{\partial^2}{\partial\theta_2^2}+\frac{\partial^2}{\partial\theta_3^2}\right)+V(\theta_1,\theta_2,\theta_3) \quad (2)$$

where I_{CH_3} stands for the moment of inertia of a methyl group and $V(\theta_1,\theta_2,\theta_3)$ represents the potential energy of the internal rotation of the methyl groups. The potential term is expanded into a Fourier series of the three variables θ_1 to θ_3. We anticipate that the simultaneous interaction involving the three methyl groups is negligible and that only pairwise interactions, if any, are significant. Then, the potential energy is given by Eq. 3 under the assumption that the terms having higher order symmetries than the three fold are negligible.

$$V(\theta_1,\theta_2,\theta_3)=V_0+V_1\sum_i\cos 3\theta+V_2\sum_{i>j}\cos 3\theta_i\cos 3\theta_j+V_2'\sum_{i>j}\sin 3\theta_i\sin 3\theta_j. \quad (3)$$

The spin Hamiltonian $\mathscr{H}_S$ is given by Eq. 4 where g and T_i^F stand for the isotropic g factor and the isotropic hfcc, respectively. The anisotropy is neglected because the observed spectra appear almost isotropic.

$$\mathscr{H}_S=\mathscr{H}_{Zeeman}+\mathscr{H}_{SI}=g\beta S_zH+\frac{1}{3}\sum_{i=1}^{3}S_Z(T_i^A I_{iZ}^A+T_i^{Ea}I_{iZ}^{Eb}+T_i^{Eb}I_{iZ}^{Ea}). \quad (4)$$

The symmetrized representation of T and the nuclear spin operator I_z is given by Eqs. 5, 6, and 7 where X represents T and I_z and the suffices denote the protons of methyl group i.

$$X_i^{\mathrm{A}} = X_{i1} + X_{i2} + X_{i3} \tag{5}$$

$$X_i^{\mathrm{Ea}} = X_{i1} + \varepsilon X_{i2} + \varepsilon^* X_{i3} \tag{6}$$

$$X_i^{\mathrm{Eb}} = X_{i1} + \varepsilon^* X_{i2} + \varepsilon X_{i3} \tag{7}$$

$$\text{where } \varepsilon = \exp(2\pi i/3). \tag{8}$$

Since all the elements of G_{27} are even permutations of the protons, the total wave function, i.e., the product of the electronic, vibrational, internal-rotational, nuclear and electron spin parts must be totally symmetric. The electronic and the vibrational ground states are totally symmetric in the G_{27} group. The electron spin function is also totally symmetric with respect to the nuclear permutation. Thus, the product of the internal-rotational (ROT) and the nuclear spin (NS) functions must be totally symmetric.[1] The product is designated as, e.g.,$|\mathrm{ROT};\ \mathrm{AAEa}\rangle|\mathrm{NS};\mathrm{AAEb};m_{\mathrm{I}}^1 m_{\mathrm{I}}^2 m_{\mathrm{I}}^3\rangle$. The nuclear spin part is further factored as in Eq. 9, for example.

$$|\mathrm{NS};\mathrm{AAEb};m_{\mathrm{I}}^1 m_{\mathrm{I}}^2 m_{\mathrm{I}}^3\rangle = |\mathrm{A}m_{\mathrm{I}}^1\rangle|\mathrm{A}m_{\mathrm{I}}^2\rangle\,|\,\mathrm{Eb}m_{\mathrm{I}}^3\rangle \tag{9}$$

The explicit forms of the component function for each methyl group are given in Eq. 10. The functions $|\mathrm{A}\ -3/2\rangle$, $|\mathrm{A}\ -1/2\rangle$, $|\mathrm{Ea}\ -1/2\rangle$, $|\mathrm{Eb}\ -1/2\rangle$ are obtained from those in Eq. 10 by exchanging α and β.

$$\begin{aligned}
|\,\mathrm{A}3/2\rangle &= |\,\alpha\alpha\alpha\rangle \\
|\,\mathrm{A}1/2\rangle &= \frac{1}{\sqrt{3}}\{|\,\beta\alpha\alpha\rangle + |\,\alpha\beta\alpha\rangle + |\,\alpha\alpha\beta\rangle\} \\
|\,\mathrm{Ea}1/2\rangle &= \frac{1}{\sqrt{3}}\{|\,\beta\alpha\alpha\rangle + \varepsilon\,|\,\alpha\beta\alpha\rangle + \varepsilon^*\,|\,\alpha\alpha\beta\rangle\} \\
|\,\mathrm{Eb}1/2\rangle &= \frac{1}{\sqrt{3}}\{|\,\beta\alpha\alpha\rangle + \varepsilon^*\,|\,\alpha\beta\alpha\rangle + \varepsilon\,|\,\alpha\alpha\beta\rangle\}
\end{aligned} \tag{10}$$

The first two functions in Eq. 10 are associated with the total nuclear spin quantum number $I^i=3/2$ for methyl group i while the latter two with $I^i=1/2$.

Hyperfine Structure at High Temperatures. The hyperfine structure of ESR spectrum is determined by the eigenstate of the Hamiltonian in Eq. 1. The energies of the internal rotation and the hyperfine interaction corresponding to the first and the second terms of the Hamiltonian in Eq. 1 are generally in the order of GHz and several tens of MHz, respectively. Therefore, we ignore the hyperfine interaction between different states of the internal rotation. Then, the overall hyperfine structure will be determined by superposing the hyperfine-structured low-lying rotational levels which are assumed to be equally populated at the temperatures studied. The basis function for the rotational part, $|\mathrm{ROT};\Gamma_1\Gamma_2\Gamma_3\rangle$, is chosen to be the eigenfunctions of the first term of Eq. 1. Within the same rotational state the first term of the hyperfine Hamiltonian in Eq. 4, i.e., $\frac{1}{3}\sum_{i=1}^{3} S_{\mathrm{z}} T_i^{\mathrm{A}} I_{iz}^{\mathrm{A}}$, is diagonal with respect to the nuclear spin functions in Eq. 9 while the remaining terms, i.e., $\frac{1}{3}\sum_{i=1}^{3} S_{\mathrm{z}}(T_i^{\mathrm{Ea}} I_{iz}^{\mathrm{Eb}} + T_i^{\mathrm{Eb}} I_{iz}^{\mathrm{Ea}})$, yield off-diagonal matrix elements. The energy of the diagonal parts of Eq. 1 is given as in Eq. 11 for the state of $|\mathrm{ROT};\Gamma_1\Gamma_2\Gamma_3\rangle|\mathrm{NS};\Gamma_1'\Gamma_2'\Gamma_3';m_{\mathrm{I}}^1 m_{\mathrm{I}}^2 m_{\mathrm{I}}^3\rangle$.

$$E_{\mathrm{R}} + E_{\mathrm{hf}} = E_{\mathrm{R}} + S_Z t(m_{\mathrm{I}}^1 + m_{\mathrm{I}}^2 + m_{\mathrm{I}}^3) \tag{11}$$

$$\text{where } t = \langle \mathrm{ROT};\Gamma_1\Gamma_2\Gamma_3 \,|\, T_1^{\mathrm{A}} \,|\, \mathrm{ROT};\Gamma_1\Gamma_2\Gamma_3\rangle \tag{12}$$

Except for the single rotational state of AAA symmetry type all the other states are degenerate in the regime of E_{R}, i.e., six-fold for AAEa, six-fold for AEaEa, six-fold for AEaEb, two-fold for EaEaEa, and six-fold for EaEaEb symmetries. The degree of degeneracy for the energy of $E_{\mathrm{R}}+E_{\mathrm{hf}}$ is summarized in Table 1 where the columns AAA through EaEaEb are for the rotational energy and the rows for the hyperfine interaction with the total sum in the last column. The sum shows the binomial distribution and corresponds to the intensity distribution of ESR spectrum at high temperatures where the off-diagonal matrix elements of the Hamiltonian in Eq. 1 are averaged out.[2]

Hyperfine Structure at Low Temperatures. Case I. At low temperatures off-diagonal matrix elements of the hyperfine interaction lift the degeneracy of states having the same energy of $E_{\mathrm{R}}+E_{\mathrm{hf}}$. For the off-diagonal matrix element to be non-zero the two states must share in common two out of the three symmetry species Γ_i's and all the three m_{I}^is must be the same. This is because the terms of $\mathscr{H}_{\mathrm{s}}$ in Eq. 4 operate on the individual methyl group and the nuclear spin operator I_{iz}^{Γ} does not change the eigenvalue of m_{I}^i. To give an explicit example, the state $|\mathrm{ROT};\mathrm{EaEaEb}\rangle|\mathrm{NS};\mathrm{EbEbEa};1/2,-1/2,1/2\rangle$ may have a non-zero matrix element with $|\mathrm{ROT};\mathrm{EaEbEb}\rangle|\mathrm{NS};\mathrm{EbEaEa};1/2,-1/2,1/2\rangle$, but there cannot be a non-zero matrix element between $|\mathrm{ROT};\mathrm{EaEbEa}\rangle|\mathrm{NS};\mathrm{EbEaEb};1/2,-1/2,1/2\rangle$ and $|\mathrm{ROT};\mathrm{EaEbEb}\rangle|\mathrm{NS};\mathrm{EbEaEa};-1/2,1/2,1/2\rangle$.

For the rotationally degenerate states of AAEa symmetry type the matrix for Eq. 1 is represented by Matrix I where the degenerate diagonal matrix elements are omitted and the off-diagonal matrix element α is given by Eq. 13.

Table 1. Degeneracy of the Energy of $E_{\mathrm{R}}+E_{\mathrm{hf}}$

$\sum_{i=1}^{3} m_{\mathrm{I}}^i$	AAA	AAEa	AEaEa	AEaEb	EaEaEa	EaEaEb	Sum
9/2	1						1
7/2	3	6					9
5/2	6	18	6	6			36
3/2	10	30	18	18	2	6	84
1/2	12	42	24	24	6	18	126
−1/2	12	42	24	24	6	18	126
−3/2	10	30	18	18	2	6	84
−5/2	6	18	6	6			36
−7/2	3	6					9
−9/2	1						1

$$\begin{matrix}|\mathrm{ROT;EaAA}\rangle|\mathrm{NS;EbAA};\pm 1/2 m_\mathrm{I}^2 m_\mathrm{I}^3\rangle \\ |\mathrm{ROT;EbAA}\rangle|\mathrm{NS;EaAA};\pm 1/2 m_\mathrm{I}^2 m_\mathrm{I}^3\rangle\end{matrix}\begin{pmatrix}\alpha^* \\ \alpha\end{pmatrix}\times S_\mathrm{Z} \quad \text{(I)}$$

$$\alpha=1/3\langle \mathrm{ROT;EbAA}|T_1^{\mathrm{Ea}}|\mathrm{ROT;EaAA}\rangle\langle E\mathrm{a}\pm 1/2|I_{1z}^{\mathrm{Eb}}|E_\mathrm{b}\pm 1/2\rangle \quad (13)$$

The two rotationally degenerate states are split into a doublet with the energies of $\pm|\alpha|$. The off-diagonal matrix elements between the rotationally degenerate states of symmetry types of AEaEa–AEbEb, AEaEb–AEbEa, and EaEaEa–EbEbEb are zero. The matrix for the states of the symmetry of EaEaEb type is given by Matrix II with the off-diagonal element of β in Eq. 14. The eigenvalues are obtained as $\pm|\beta|$ (doubly degenerate) and $\pm 2|\beta|$.

$$\begin{matrix}|\mathrm{ROT;EaEaEb}\rangle|\mathrm{NS;EbEbEa};m_\mathrm{I}^1 m_\mathrm{I}^2 m_\mathrm{I}^3\rangle \\ |\mathrm{ROT;EaEbEa}\rangle|\mathrm{NS;EbEaEb};m_\mathrm{I}^1 m_\mathrm{I}^2 m_\mathrm{I}^3\rangle \\ |\mathrm{ROT;EbEaEa}\rangle|\mathrm{NS;EaEbEb};m_\mathrm{I}^1 m_\mathrm{I}^2 m_\mathrm{I}^3\rangle \\ |\mathrm{ROT;EbEbEa}\rangle|\mathrm{NS;EaEaEb};m_\mathrm{I}^1 m_\mathrm{I}^2 m_\mathrm{I}^3\rangle \\ |\mathrm{ROT;EbEaEb}\rangle|\mathrm{NS;EbEaEa};m_\mathrm{I}^1 m_\mathrm{I}^2 m_\mathrm{I}^3\rangle \\ |\mathrm{ROT;EaEbEb}\rangle|\mathrm{NS;EbEaEa};m_\mathrm{I}^1 m_\mathrm{I}^2 m_\mathrm{I}^3\rangle\end{matrix}\begin{pmatrix} & & & & & \beta^*\beta^* \\ & & & & \beta^* & \beta^* \\ & & & \beta^*\beta^* & & \\ & & \beta\beta & & & \\ & \beta & \beta & & & \\ \beta\beta & & & & & \end{pmatrix}\times S_z \quad \text{(II)}$$

$$\beta = 1/3\langle \mathrm{ROT;EbEaEb}|T_1^{\mathrm{Ea}}|\mathrm{ROT;EaEaEb}\rangle \langle \mathrm{Ea}\pm 1/2|I_{1z}^{\mathrm{Eb}}|\mathrm{Eb}\pm 1/2\rangle \quad (14)$$

We now evaluate the matrix elements of $\mathscr{H}_\mathrm{s}$, i.e., t, α, and β. For the evaluation of the rotational part the wavefunction of the methyl protons is regarded as localized at the local minima of potential. Then, the isotropic hfcc is approximated by Eq. 15,

$$T_{ij} = 2B\cos^2\phi_{ij}, \quad (15)$$

where B stands for the average of the hfcc's of the three protons and ϕ is the angle between the 2p orbital of carbon and the CH bond and the suffices i and j specify the j-th proton of the i-th methyl group. With this approximation the following relations are obtained where the bracket means the expectation value with respect to the rotational function and the angle ϕ corresponds to the potential minimum for proton 1.[2)]

$$t = \langle T_i^\mathrm{A}\rangle \cong B \quad (16)$$

$$\langle T_i^{\mathrm{Ea}}\rangle I_{iz}^{\mathrm{Eb}} \cong \frac{3}{2}B\mathrm{e}^{2i\phi}I_{iz}^{\mathrm{Eb}} \quad (17)$$

The evaluation of the nuclear spin part is straightforward with the use of the symmetrized spin functions in Eq. 10 and the symmetrized operators in Eqs. 5, 6, and 7. The matrix elements α and β are, thus, obtained as in Eq. 18 with the signs + and − corresponding, respectively, to $m_\mathrm{I}^1=-1/2$ and $+1/2$.[1,2,4)]

$$\alpha = \beta = \pm\frac{B}{2}\mathrm{e}^{2i\phi} \quad (18)$$

Scheme 1 shows the ESR pattern to be expected at low temperatures. The scheme is derived from Table 1 by introducing the splittings due to α and β. The states of AAEa symmetry type having the same value of $m_\mathrm{I}^1+m_\mathrm{I}^2+m_\mathrm{I}^3$ are split into a doublet with the separation of $\pm|\alpha|=\pm B/2$. Likewise, the four states of EaEaEb symmetry type split into a quintet with the intensity ratio of 1 : 2 : 0 : 2 : 1 and the spacing of $|\beta|=B/2$. The total nineteen levels shown at the bottom of Scheme 1 have an equal spacing of $B/2$.

Hyperfine Structure at Low Temperatures. Case II. The above result is based on the assumption that the energy difference of the internal rotation is much larger than that of the hyperfine interaction and we have considered the lifting of the degeneracy of the sum of $E_\mathrm{R}+E_\mathrm{hf}$ by the hyperfine interaction. However, there is a possibility of a degeneracy in the rotational states by themselves in which case the hyperfine structural pattern in Scheme 1 will be altered to that in Scheme 2 given below. In the following we will examine such a case.

In the potential function of Eq. 3 the interaction between the methyl groups i and j can be rewritten as in Eq. 19.

$$V_2\cos 3\theta_i\cos 3\theta_j + V_2'\sin 3\theta_i\sin 3\theta_j = 1/2(V_2-V_2')\cos 3(\theta_i+\theta_j)+1/2(V_2+V_2')\cos 3(\theta_i-\theta_j). \quad (19)$$

The first and the second terms in the right hand side of Eq. 19 correspond to the potentials for the conrotation and the disrotation of methyl groups i and j. Now, in case of $V_2'=0$, the barriers for the two modes of rotation are equal so that the six states of AEaEa symmetry type and another six of AEaEb type become degenerate.[4)] Similarly, the two states of EaEaEa type and the six of EaEaEb are degenerate to form a set of eight states of EEE type. For the reason stated in connection with Matrix I the non-zero off-diagonal elements in the Hamiltonian matrix for the states of AEE type appear as in Matrix III.

$$\begin{matrix}|\mathrm{ROT;EaEaA}\rangle \\ |\mathrm{ROT;EbEbA}\rangle \\ |\mathrm{ROT;EaEbA}\rangle \\ |\mathrm{ROT;EbEaA}\rangle\end{matrix}\begin{pmatrix} & & \gamma^*\gamma^* \\ & & \gamma\ \gamma \\ \gamma\gamma^* & & \\ \gamma\gamma^* & & \end{pmatrix}\times S_\mathrm{z} \quad \text{(III)}$$

$$\gamma = 1/3\langle \mathrm{ROT;EbEaA}|T_1^{Ea}|\mathrm{ROT;EaEaA}\rangle \langle \mathrm{Ea}\pm 1/2|I_{1z}^{\mathrm{Eb}}|\mathrm{Eb}\pm 1/2\rangle \quad (20)$$

The eigenvalues of Matrix III are 0 (doubly degenerate) and $\pm 2|\gamma|$. Similarly, the 6×6 matrix for the EaEaEb type (Matrix II) is expanded to the following 8×8 matrix with the additional non-zero off-diagonal element δ given in Eq. 21.

AAA	1		3		6		10		12		12		10		6		3		1
AAEa		3		12		24		36		42		36		24		12		3	
AEaEa					6		18		24		24		18		6				
AEaEb					6		18		24		24		18		6				
EaEaEa							2		6		6		2						
EaEaEb					1	2	3	8	4	12	4	8	3	2	1				
Total	1	3	3	12	19	26	51	44	70	54	70	44	51	26	19	12	3	3	1

Scheme 1.

AAA	1		3		6		10		12		12		10		6		3		1
AAE		3		12		24		36		42		36		24		12		3	
AEE			3		15		33		45		45		33		15		3		
EEE				1		6		15		20		15		6		1			
Total	1	3	6	13	21	30	43	51	57	62	57	51	43	30	21	13	6	3	1

Scheme 2.

$$\begin{array}{l}
|\mathrm{ROT;EaEaEa}\rangle|\mathrm{NS;EbEbEb};m_{\mathrm{I}}^1 m_{\mathrm{I}}^2 m_{\mathrm{I}}^3\rangle \\
|\mathrm{ROT;EbEbEb}\rangle|\mathrm{NS;EaEaEa};m_{\mathrm{I}}^1 m_{\mathrm{I}}^2 m_{\mathrm{I}}^3\rangle \\
|\mathrm{ROT;EaEaEb}\rangle|\mathrm{NS;EbEbEa};m_{\mathrm{I}}^1 m_{\mathrm{I}}^2 m_{\mathrm{I}}^3\rangle \\
|\mathrm{ROT;EaEbEa}\rangle|\mathrm{NS;EaEbEb};m_{\mathrm{I}}^1 m_{\mathrm{I}}^2 m_{\mathrm{I}}^3\rangle \\
|\mathrm{ROT;EbEaEa}\rangle|\mathrm{NS;EaEbEb};m_{\mathrm{I}}^1 m_{\mathrm{I}}^2 m_{\mathrm{I}}^3\rangle \\
|\mathrm{ROT;EbEbEa}\rangle|\mathrm{NS;EaEaEb};m_{\mathrm{I}}^1 m_{\mathrm{I}}^2 m_{\mathrm{I}}^3\rangle \\
|\mathrm{ROT;EbEaEb}\rangle|\mathrm{NS;EbEaEa};m_{\mathrm{I}}^1 m_{\mathrm{I}}^2 m_{\mathrm{I}}^3\rangle \\
|\mathrm{ROT;EaEbEb}\rangle|\mathrm{NS;EbEaEa};m_{\mathrm{I}}^1 m_{\mathrm{I}}^2 m_{\mathrm{I}}^3\rangle
\end{array}
\begin{pmatrix}
\delta^*\delta^*\delta^* & & & & & & & \\
 & & & \delta & \delta & \delta & & \\
\delta & & & & & \beta^*\beta^* & & \\
\delta & & & & \beta^* & & \beta^* & \\
\delta & & & & \beta^*\beta^* & & & \\
 & \delta^* & \beta & \beta & & & & \\
 & \delta^*\beta & & \beta & & & & \\
 & \delta^*\beta & \beta & & & & &
\end{pmatrix} \times S_z \quad \text{(IV)}$$

$$\delta = 1/3\langle \mathrm{ROT;EbEaEa}|\, T_1^{\mathrm{Ea}}|\mathrm{ROT;EaEaEa}\rangle \langle \mathrm{Ea}\pm 1/2|I_{1z}^{\mathrm{Eb}}|\mathrm{Eb}\pm 1/2\rangle \quad (21)$$

Application of the same approximation which has led to Eq. 15 gives the following equation where the signs + and − correspond to $m_{\mathrm{I}}^1 = -1/2$ and $+1/2$, respectively.

$$\alpha = \beta = \gamma = \delta = \pm\frac{B}{2}e^{2i\phi}. \quad (22)$$

The eight eigenvalues of Matrix IV are $\pm B/2$ (triply degenerate) and $\pm 3B/2$.

The above splittings caused by the off-diagonal matrix elements γ and δ lead to a different spectral pattern, i.e., the sum of the degree of degeneracy of AEaEa and AEaEb types having the same value of $\sum_i m_{\mathrm{I}}^i$ (see Table 1) will be split into a triplet with the intensity ratio of 1 : 2 : 1 and with the separation of $2|\gamma| = B$. The resultant intensity distribution is given in the third row of Scheme 2 below. Similarly, the sum of EaEaEa and EaEaEb types having the same value of $\sum_i m_{\mathrm{I}}^i$ will be split into a quartet with the ratio of 1 : 3 : 3 : 1 and the spacing of B as summarized in the fourth row of Scheme 2. The total nineteen levels given in the fifth row of Scheme 2 are equally spaced by $B/2$.

Comparison of Cases I and II with the Experimental Spectrum. Comparison of the last rows of Schemes 1 and 2 indicates that the ESR spectrum at low temperatures differs depending upon whether V_2' is zero or not. Since the central part of the observed spectrum is overshadowed by the signal due to the CD_2OD radical, the comparison has to be made for the outer part of the spectrum. It seems obvious that Scheme 2 reproduces the observed eight pairs of outer peaks as shown in Fig. 1, where the spectrum observed at 6.6 K is compared with the properly line-broadened simulation spectrum for Scheme 2 with the jumping parameter k (see below) being assumed to be zero. We could not reproduce by simulation the decrease in the intensity of the eighth peak (44) relative to the seventh (51) and nineth(70) peaks counted from both ends of the Total Ratio of Scheme 1 whereas the intensity of the three peaks increases monotonously in the simulation for Scheme 2, which is compatible with the observed spectrum. The result implies that the two modes of the rotation, con and dis, of any pair of the methyl groups in the *t*-butyl radical are indiscriminate.

Thermally Induced Random Rotation. The change of the ESR spectrum from the nineteen to ten lines is explained by random, spin-independent rotations;[2] if the correlation time of the random rotation is short enough compared to the ESR time scale, the off-diagonal matrix elements α,β,γ, and δ are averaged out to be nil. The intensity pattern in Table 1 corresponds to this case. The averaging can be regarded as a jumping between the states.[2] While the rotational state of AAA type is not affected by the thermal agitation, the state of AAE type is, and one parameter k_1 is needed to describe the jumping between the two sites of AAEa and AAEb. Likewise, for the AEE type three parameters k_2 and k_3, k_4 are necessary to describe the 4 site-jumps of EaEa↔EbEb, EaEa↔EaEb, and EaEb↔EbEa. Similarly, for the EEE type six parameters are required. Since there are so many parameters, the complete kinetic analysis is prohibitive. However, if we look into the details of Scheme 2, we see that the intensities of the second, fourth, and sixth lines as counted from both ends of the last row of the scheme are mainly contributed from the state of AAE type of the second row. It is these even-numbered lines which are to be broadened by the jumping. Therefore, we anticipate that the line broadening due to the jumping

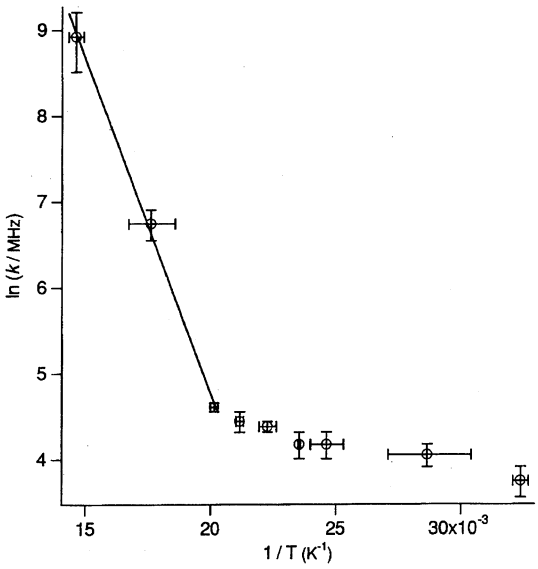

Fig. 3. Arrhenius plot for the jumping (see text).

may be approximately describable by a single parameter k_1. With this presumption the simulation for the line broadened spectra is carried out using the density matrix method by Heinzer[9] as in our previous study on the radical cation of dimethyl ether.[4] Figure 2 demonstrates the spectra observed at several temperatures and the simulated ones to reproduce the observed spectra. The overall agreement between the two columns is satisfactory.

Figure 3 shows the Arrhenius plot for the jumping. A kink is seen at about 50 K which indicates that the tunneling becomes apparent at temperatures below about 50 K.[4,10] An activation energy of 6±2 kJ mol^{-1} is estimated from the plots at temperature above 50 K.

Concluding Remark. We have studied the ESR spectrum of the *t*-butyl radical at low temperatures closely following our previous work on the radical cation of dimethyl ether to find that the hyperfine interaction lifts the degeneracy in the internal rotation regime and that the pairwise interaction of the two methyl internal rotations, if any, is describable by the potential of the form of $\cos\theta_i \cos\theta_j$, which can be rephrased as that the con and dis rotations are degenerate in energy.

The authors are indebted to Drs. Takamasa Momose and Paul J. Krusic[11] for their valuable comments. The study was partially supported by Grants-in-Aid for Scientific Research on Priority Areas No.05237105 from the Ministry of Education, Science and Culture.

References

1) J. H. Freed, *J. Chem. Phys.*, **43**, 1710 (1965).
2) S. Clough and F. Poldy, *J. Chem. Phys.*, **51**, 2076 (1969).
3) B. Davidson and I. Miyagawa, *J. Chem. Phys.*, **52**, 1727 (1970).
4) M. Matsushita, T. Momose, and T. Shida, *J. Chem. Phys.*, **92**, 4749 (1990).
5) D. E. Wood and R. F. Sprecher, *Mol. Phys.*, **26**, 1311 (1973).
6) A. A-Raqabah and M. C. R. Symons, *Chem. Phys. Lett.*, **183**, 171 (1991).
7) H. C. Longuet-Higgins, *Mol. Phys.*, **6**, 445 (1963).
8) Philip R. Bunker, "Molecular Symmetry and Spectroscopy," Academic Press, New York (1979).
9) J. Heinzer, *Mol. Phys.*, **22**, 167 (1971).
10) M. Geffroy, L. D. Kispert, and J. S. Hwang, *J. Chem. Phys.*, **70**, 4238 (1979).
11) D. Griller, K. U. Ingold, P. J. Krusic, and H. Fischer, *J. Am. Chem. Soc.*, **100**, 6750 (1978).